AJNR

Primary Intracranial Atypical Teratoid/Rhabdoid Tumors of Infancy and Childhood: MRI Features and Patient Outcomes

S.P. Meyers, Z.P. Khademian, J.A. Biegel, S.H. Chuang, D.N. Korones and R.A. Zimmerman

AJNR Am J Neuroradiol 2006, 27 (5) 962-971
http://www.ajnr.org/content/27/5/962

ORIGINAL RESEARCH

S.P. Meyers
Z.P. Khademian
J.A. Biegel
S.H. Chuang
D.N. Korones
R.A. Zimmerman

Primary Intracranial Atypical Teratoid/Rhabdoid Tumors of Infancy and Childhood: MRI Features and Patient Outcomes

BACKGROUND AND PURPOSE: Primary atypical teratoid/rhabdoid tumors (AT/RTs) are rare malignant intracranial neoplasms, usually occurring in young children. The objectives of this study were to characterize the MR imaging features and locations of primary intracranial AT/RTs, to determine the frequency of disseminated disease in the central nervous system (CNS) at diagnosis and postoperatively, and to assess patient outcomes.

METHODS: The preoperative cranial MR images of 13 patients with AT/RTs were retrospectively reviewed for evaluation of lesion location, size, MR signal intensity and enhancement characteristics, and the presence of disseminated intracranial tumor. Postoperative MR images of the head and spine for 17 patients were reviewed for the presence of locally recurrent or residual tumor and disseminated neoplasm. Imaging data were correlated with patient outcomes.

RESULTS: Patients ranged in age from 4 months to 15 years (median age, 2.9 years). Primary AT/RTs were intra-axial in 94% of patients. The single primary extra-axial lesion was located in the cerebellopontine angle cistern. AT/RTs were infratentorial in 47%, supratentorial in 41%, and both infra- and supratentorial in 12%. A germ-line mutation of the hSNF5/INI1 tumor-suppressor gene was responsible for the simultaneous occurrence of an intracranial AT/RT and a malignant renal rhabdoid tumor in a 4-month-old patient. Mean tumor sizes were $3.6 \times 3.8 \times 3.9$ cm. On short TR images, AT/RTs typically had heterogeneous intermediate signal intensity, as well as zones of low (54%), high (8%), or both low and high (31%) signal intensity from cystic and/or necrotic regions, hemorrhage, or both, respectively. On long TR/long TE images, solid portions of AT/RTs typically had heterogeneous intermediate-to-slightly-high signal intensity with additional zones of high (54%) or both high and low signal intensity (38%), secondary to cystic and/or necrotic regions, edema, prior hemorrhage, and/or calcifications. AT/RT had isointense and/or slightly hyperintense signal intensity relative to gray matter on fluid-attenuated inversion-recovery (FLAIR) and long TR/long TE images, and showed restricted diffusion. All except 1 AT/RT showed contrast enhancement. The fraction of tumor volume showing enhancement was greater than two thirds in 58%, between one third and two thirds in 33%, and less than one third in 9%. Disseminated tumor in the leptomeninges was seen with MR imaging in 24% of patients at diagnosis/initial staging and occurred in another 35% from 4 months to 2.8 years (mean, 1.1 years) after surgery and earlier imaging examinations with negative findings. The overall 1-year and 5-year survival probabilities were 71% and 28%, respectively. Patients with MR imaging evidence of disseminated leptomeningeal tumor had a median survival rate of 16 months compared with 149 months for those without disseminated tumor ($P < .004$, logrank test).

CONCLUSION: AT/RTs are typically intra-axial lesions, which can be infra- and/or supratentorial. The unenhanced and enhanced MR imaging features of AT/RT are often variable secondary to cystic/necrotic changes, hemorrhage, and/or calcifications. Poor prognosis is associated with MR imaging evidence of disseminated leptomeningeal tumor.

Primary atypical teratoid/rhabdoid tumors (AT/RTs) are rare malignant intracranial neoplasms usually occurring in young children.[1-13] They were termed "AT/RT" because they contain nests or sheets of rhabdoid tumor cells as well as varying proportions of primitive neuroectodermal tumor (PNET) cells, mesenchymal spindle-shaped tumor cells, and/or epithelial-type tumor cells.[1,3,7,8,11,12] AT/RT has been misdiagnosed in the past as PNET because of frequent overlapping histologic features.[1,3-6] AT/RTs can now be distinguished from PNET and other tumors by using specific immunohistochemical markers and by detection of deletions and/or mutations involving the hSNF5/INI1 tumor-suppressor gene in chromosome band 22q11.2.[1,3-10] These tumors have aggressive growth with high potential for dissemination within the central nervous system (CNS).[1-13] Confirmation of the diagnosis of AT/RT is important because the tumors typically have a poor prognosis that is worse than that of PNET/medulloblastoma (MB), necessitating intensive therapy that differs markedly from the treatment for PNET/MB.[1,3,4,9,10]

The objectives of this study were to characterize the MR imaging features and locations of primary intracranial AT/RT, to determine the frequency of disseminated disease in the CNS at diagnosis and during postoperative surveillance MR imaging, and to assess patient outcomes.

Received July 13, 2005; accepted after revision October 10.

From the Departments of Radiology (S.P.M.) and Pediatrics (D.N.K.), University of Rochester School of Medicine, Strong Memorial Hospital, Rochester, NY; Departments of Radiology (Z.P.K., R.A.Z.) and Pathology and Pediatrics (J.A.B.), Children's Hospital of Philadelphia and University of Pennsylvania School of Medicine, Philadelphia, Pa; and the Department of Radiology (S.H.C.), Hospital for Sick Children, Toronto, Ont, Canada.

Please address correspondence to: Steven P. Meyers, MD, PhD, Department of Radiology, P.O. Box 648, University of Rochester Medical Center, 601 Elmwood Ave, Rochester, NY 14642.

Table 1: Clinical data of 17 patients with atypical teratoid/rhabdoid tumors

Patient No./ Age (y)/Sex	Tumor Location	Surgical Resection or Biopsy	Disseminated Tumor at Diagnosis/MRI	CSF Cytology at Diagnosis	Postoperative Treatment	Outcome
1/2/F	Vermis	Total	−	−	R+C	Dead
2/4/M	Vermis	Total	−	−	R+C	No evident disease
3/10/M	Vermis	Total	−	−	R	No evident disease
4/3.2/M	Cerebellar hemisphere	Subtotal	−	−	R+C	No evident disease
5/1.3/M	Midbrain	Biopsy	+	+	C	Dead
6/0.8/F	Cerebello–pontine angle cistern	Subtotal	−	−	C	Dead
7/5/M	Frontal lobe	Partial	+	−	R+C	Dead
8/3.4/F	Frontal lobe	Subtotal	−	−	R+C	Dead
9/4/M	Frontal lobe	Partial	−	−	R+C	Dead
10/4/F	Septum pellucidum	Subtotal	−	−	R+C	Dead
11/0.7/F	Pineal	Subtotal	−	−	C	Dead
12/0.3/F	Pineal–midbrain–cerebellum	Biopsy	−	−	None	Dead
13/0.8/M	Pineal–midbrain–cerebellum	Biopsy	+	+	None	Dead
14/6/F	Vermis	Total	+	−	R+C	Dead
15/15/M	Frontal lobe	Total	−	−	R+C	No evident disease
16/0.5/M	Pineal	Total	−	−	C	Dead
17/2.5/M	Cervical–medullary junction	Partial	−	−	C	Dead

Note:—CSF indicates cerebrospinal fluid; R, radiation therapy; C, chemotherapy.

Methods

Patient Group

We reviewed the tumor registry files and surgical and pathologic reports from 3 medical centers and found records of 17 patients who had resection of primary intracranial AT/RT from 1991 to 2001. Thirteen patients had preoperative MR imaging examinations of the head. Seventeen patients, including the 13 patients with preoperative MR imaging, had postoperative staging and surveillance MR imaging of the spine and head. The study group consisted of 10 male and 7 female patients (Table 1). At the time of diagnosis, the patients ranged in age from 4 months to 15 years (mean age, 3.7 years; median age, 2.9 years). Fifteen patients (88%) were younger than 7 years at diagnosis, including 8 who were 3 years of age or younger. By surgical report, 6 patients (35%) had gross total resection of AT/RT, 5 (29%) had subtotal resection (> 75% reduction in tumor size), 3 (18%) had partial resection (25%–75% reduction), and 3 (18%) had undergone biopsies. Five patients had undergone postoperative chemotherapy, 1 patient was treated with radiation, and 9 patients experienced both chemotherapy and radiation.

Pathology Reports

Reports from light microscopic studies by neuropathologists at the 3 institutions were reviewed for descriptions of AT/RT with regard to the presence of rhabdoid cells in the specimens as well as necrosis and hemorrhage. To distinguish AT/RT from germ-cell tumors, classic PNETs, and other primary tumors of the CNS, one routinely uses immunoreactivity to specific monoclonal antibodies (epithelial membrane antigen, vimentin, actin, desmin, cytokeratin, glial fibrillary acidic protein, and neurofilament protein) with the immunoperoxidase technique.[3] Results of reactivity of samples of AT/RT to these monoclonal antibodies were reviewed. Tumor karyotypes were available for 3 patients. Results from cytogenetic analyses for deletions involving 22q11.2 by using an interphase fluorescence in situ hybridization technique were available for 7 AT/RTs.[1,4,6] Results from molecular genetic analyses for mutations involving the hSNF5/INI1 rhabdoid tumor-suppressor gene on chromosome 22q11.2 were available for 7 patients using heteroduplex and direct sequence analysis.[4,6] Results from the immunohistochemical analysis for the gene product of the hSNF5/INI1 tumor-suppressor gene were available for 4 tumor samples.[7]

MR Imaging

MR imaging was performed at 1.5T. Thirteen patients had preoperative contrast-enhanced MR imaging of the head. Multisection spin-echo pulse images were obtained in all MR imaging of the head and included short TR/short TE (400–800/9–22/1–2 [TR/TE/excitations]), long TR/short TE (2000–3200/15–30/1–2), and long TR/long TE (2000–6000/70–132/1–3) images. Fluid-attenuated inversion recovery (FLAIR) (9000–10 000/120–148/2200 [TR/TE/TI] images were obtained in 6 patients. Echo-planar diffusion-weighted images (DWI) were obtained in 4 patients and were acquired with b values of 1000 seconds/mm^2 in 3 orthogonal gradient directions. Apparent diffusion coefficient (ADC) images were also generated to assess false-positive nondiffusion-related effects on DWI. Single-voxel ($n = 1$) and multivoxel ($n = 2$) proton MR spectroscopy was performed on 1 AT/RT before surgery and 2 residual tumors by using spin-echo point-resolved sequences (1000–1600/135–144 [TR/TE]) with volumes of interest ranging from 8 to 16 mL. MR imaging was performed in all patients after IV administration of gadopentetate dimeglumine or gadoteridol (0.1 mmol/kg) by use of short TR/short TE sequences (400–800/11–22/1–2).

The preoperative cranial MR images of AT/RTs were evaluated for location, lesion size, MR signal intensity (low, intermediate, high, or mixed), signal intensity relative to gray matter on FLAIR and long TR/long TE images, contrast-enhancement features (degree: mild, moderate, or prominent; extent: small [less than one third], intermediate [one third to two thirds], or large [more than two thirds]; and pattern: heterogeneous or homogeneous). The presence of disseminated disease in the leptomeninges at diagnosis was assessed. Signal intensity of AT/RTs on DWI and ADC images was compared with that in noninvolved portions of brain parenchyma. Preoperative CT scans were also available for review for 6 patients.

A total of 65 contrast-enhanced postoperative MR imaging studies of the spine and 121 contrast-enhanced postoperative MR imaging studies of the head were reviewed. The unenhanced and contrast-enhanced postoperative short TR images of the spine were evaluated

Table 2: Immunohistochemical features of atypical teratoid/rhabdoid tumors

Antibody	% Positive
Epithelial membrane antigen	100
Vimentin	100
Actin	83
Cytokeratin	75
Desmin	23
Glial fibrillary acidic protein	87
Neurofilament protein	50

for enhancement in the pial-subarachnoid space. Postoperative MR images of the head were evaluated for lesions or abnormal enhancement in the brain parenchyma, ventricles, leptomeninges, and dura. All MR images were reviewed by 2 neuroradiologists with subsequent correlation to the reports of the examinations from each institution.

CSF Cytologic Analysis

Results from CSF histopathologic examinations were available for 15 of the 17 patients. A total of 54 CSF samples were obtained after surgery. Thirty-three of the CSF samples were contemporaneous with MR imaging (ie, obtained within 3 weeks of MR imaging examinations; mean, 7.2 days; median, 5 days). Results of CSF histopathologic analysis were compared with those of contemporaneous MR imaging examinations in the assessment for disseminated leptomeningeal tumor and patient outcomes.

Statistical Methods

The dates of patients' deaths were correlated with the initial surgical dates and those of postoperative MR imaging results positive for locally recurrent and disseminated tumor. The intervals between the dates of last contact for patients without and with recurrent and/or disseminated disease and initial surgery were also determined. Progression-free survival (PFS) and 5-year survival probabilities were calculated. Distributions of PFS and 5-year survival probabilities were estimated by using the Kaplan-Meier method.[14]

Results

Information pertaining to case demographic and clinical data are given in Table 1. Tables 2 and 3 list the immunoreactivity profiles and imaging findings of AT/RT, respectively.

Pathologic Findings

All specimens of AT/RT had histologic evidence of rhabdoid cells. Necrosis and hemorrhage were described in the reports of 10 and 4 lesions, respectively. Immunoreactivity results of tumor specimens to monoclonal antibodies are listed in Table 2. Positive reactions of antibodies to vimentin, epithelial membrane antigen (EMA), and actin (which are 3 epitopes typically expressed by rhabdoid tumor cells in AT/RT) were observed in 100%, 100%, and 83%, respectively. Reactivity to the primary neural antibodies, neurofilament protein (NFP), and glial fibrillary acidic protein (GFAP) was observed in 50% and 87%, respectively. Monosomy of chromosome 22 was found in 2 of 3 AT/RTs tested for tumor karyotypes. The other patient had a constitutional ring chromosome 22 with loss of the distal part of the long arm containing the 22q11.2 locus. Deletions and/or mutations of the tumor-suppressor gene hSNF5/INI1 in chromosome 22 were found in all 7 AT/RTs tested. In addition, 3 patients had germ-line mutations involving the hSNF5/INI1 gene, including a 4-month-old patient who had synchronous intracranial AT/RT and a malignant rhabdoid tumor in the left kidney. The intracranial tumor showed immunoreactivity to GFAP and NFP, whereas the malignant renal rhabdoid tumor did not. All 4 AT/RTs tested showed no nuclear staining for the hSNF5/INI1 gene product, indicating inactivation of both hSNF5/INI1 tumor-suppressor genes.

Tumor Location

The locations of AT/RTs are listed in Table 1. Eight (47%) of AT/RTs were infratentorial (Figs 1–3), 7 (41%) were supratentorial (Figs 4, 5)), and 2 were both infra- and supra-

Table 3: Preoperative MR imaging data of 13 patients with atypical teratoid/rhabdoid tumors

Patient No./ Age (y)/Sex	Tumor Location	Tumor Size (cm)	Hemorrhage	Cyst/Necrosis	Long TR/ Long TE (T2WI)	FLAIR	ADC	Postgadolinium
1/2/F	Vermis	3 ×3 .2 × 3.5	−	+	1+			3+/heterogeneous
2/4/M	Vermis	4 × 4 × 3.4	−	+	1+	iso	Decreased	2+/heterogeneous
3/10/M	Vermis	3.8 × 4 × 3.8	+	+	1+			1+/heterogeneous
4/3.2/M	Cerebellar hemisphere	2.8 × 3.8 × 3	−	+	iso	iso, 1+		3+/heterogeneous
5/1.3/M	Midbrain	1.2 × 1.3 × 1.2	−	−	1+	1+		3+/homogeneous
6/0.8/F	Cerebello–pontine angle cistern	3 × 3.2 × 3	−	+	iso			3+/heterogeneous
7/5/M	Frontal lobe	6 × 6.5 × 9	+	+	iso	iso		3+/heterogeneous
8/3.4/F	Frontal lobe	5.2 × 4.8 × 6	−	+	iso	iso	Decreased	3+/heterogeneous
9/4/M	Frontal lobe	4.2 × 7 × 6.5	+	+	iso			3+/heterogeneous
10/4/F	Septum pellucidum	3.8 × 3.4 × 3.8	−	+	iso			1+/heterogeneous
11/0.7/F	Pineal	2 × 2 × 2.5	+	+	1+	iso	Decreased	none
12/0.3/F	Pineal–midbrain–cerebellum	4 × 3 × 2.2	+	+	1+		Decreased	1+/heterogeneous
13/0.8/M	Pineal–midbrain–cerebellum	3.5 × 2.8 × 2.8	−	+	1+			3+/heterogeneous

Note:—Signal intensity on T2WI and FLAIR refers signal of atypical teratoid/rhabdoid tumors relative to gray matter with iso (isointense) indicating the same as and 1+ and 2+ being progressively higher in signal. Apparent diffusion coefficient (ADC) of the atypical teratoid/rhabdoid tumors is listed relative to normal uninvolved gray matter. For postgadolinium contrast enhancement, *none* indicates no enhancement and 1+, 2+, and 3+ represent progressively greater degrees of enhancement.

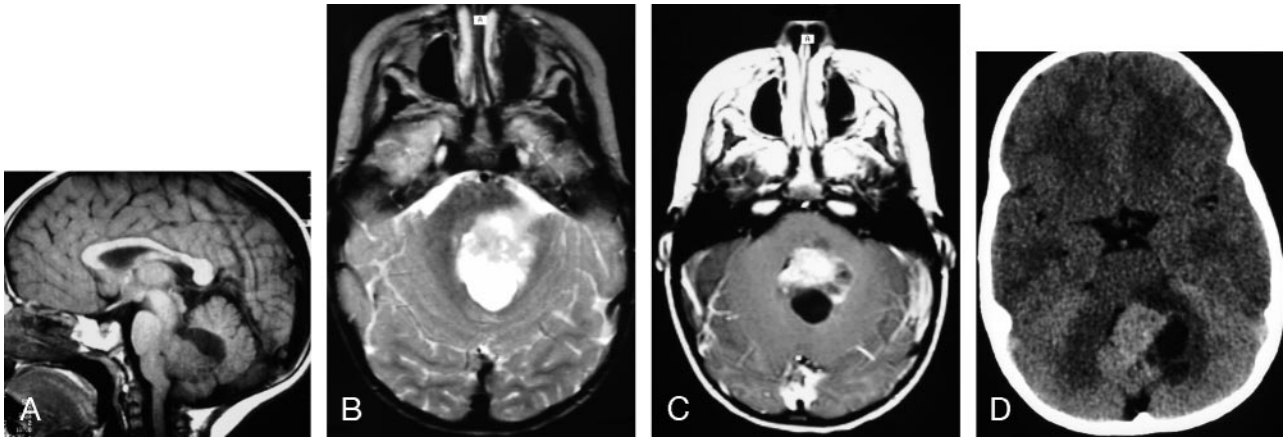

Fig 1. MR images of a 2-year-old girl with a germ-line mutation of the hSNF5/INI1 gene and AT/RT in the vermis extending into the fourth ventricle.

A, Sagittal (TR/TE, 520/10) MR image shows the tumor to have intermediate and low signal intensity. The tumor invades the dorsal brain stem.

B, Axial (TR/TE, 5700/90) MR image shows the tumor to have heterogeneous intermediate-to-slightly-high signal intensity that is slightly hyperintense relative to gray matter, as well as zones of high signal intensity representing cystic/necrotic regions. Abnormal high signal intensity is also seen in the dorsal pons and left middle cerebellar peduncle, consistent with tumor invasion.

C, Axial (TR/TE, 680/22) MR image shows the tumor to have solid-enhancing and nonenhancing cystic/necrotic components. Irregular enhancing margins of the lesion are seen at the dorsal pons and left middle cerebellar peduncle, consistent with tumor invasion. This patient died 1.6 years after diagnosis from locally recurrent and disseminated tumor.

D, Axial CT image shows the solid portion of the AT/RT to have attenuation slightly higher than that of gray matter. Low-attenuation cystic/necrotic zones and several tiny calcifications are also present.

Fig 2. MR images of a 10-year-old boy with AT/RT in the vermis, extending into the fourth ventricle.

A, Axial (TR/TE, 600/11) MR image shows the tumor to have mixed intermediate signal intensity as well as irregular zones of high signal intensity secondary to hemorrhage (methemoglobin).

B, Axial (TR/TE, 3500/108) MR image shows the tumor to have heterogeneous mixed low, intermediate, and high signal intensity.

C, Axial (TR/TE, 500/29) MR image shows contrast enhancement in less than two thirds of the AT/RT. This patient is alive without evidence of disease 9 years after surgery/initial diagnosis.

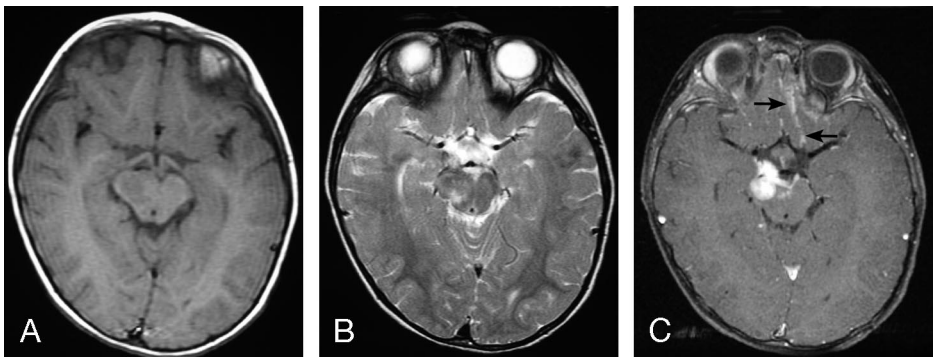

Fig 3. MR images of a 1.3-year-old boy with AT/RT in the right cerebral peduncle.

A, Axial (TR/TE, 600/10) MR image shows the tumor to have intermediate signal intensity.

B, Axial (TR/TE, 4000/105) MR image shows the tumor to have heterogeneous intermediate-to-slightly-high signal intensity, which includes zones that are isointense or slightly hyperintense to gray matter.

C, Axial (TR/TE, 700/22) fat-suppressed MR image shows prominent homogeneous contrast enhancement of the primary lesion as well as abnormal subarachnoid enhancement in the interpeduncular cistern and along the sulci adjacent to frontal lobes (*arrows*), representing disseminated leptomeningeal tumor. This patient died 4 months after diagnosis.

tentorial (12%) via contiguous extension (Fig 6). The cerebellum was the most frequent infratentorial location. The 2 lesions that were both infra- and supratentorial primarily involved the pineal gland and dorsal midbrain, with some extension into the cerebellum (Fig 6). Of the supratentorial lesions, the frontal lobe was the most frequent site (Fig 4). AT/RT is typically intra-axial (94%) except for 1 extra-axial lesion located in the cerebellopontine angle cistern (Fig 7). At surgery, the extra-axial lesion was found to extend into the porus acousticus and was adherent to the dura laterally, the seventh and eighth cranial nerves inferiorly, and the brain stem medially. Intraventricular extension of primary AT/RT was found into the third ventricle ($n = 1$), fourth ventricle ($n = 3$), third and fourth ventricles ($n = 2$), and lateral ventricle ($n = 1$) (Figs 1, 2, 5, and 6). At the time of diagnosis and initial staging, 4 (24%) of 17 patients had MR im-

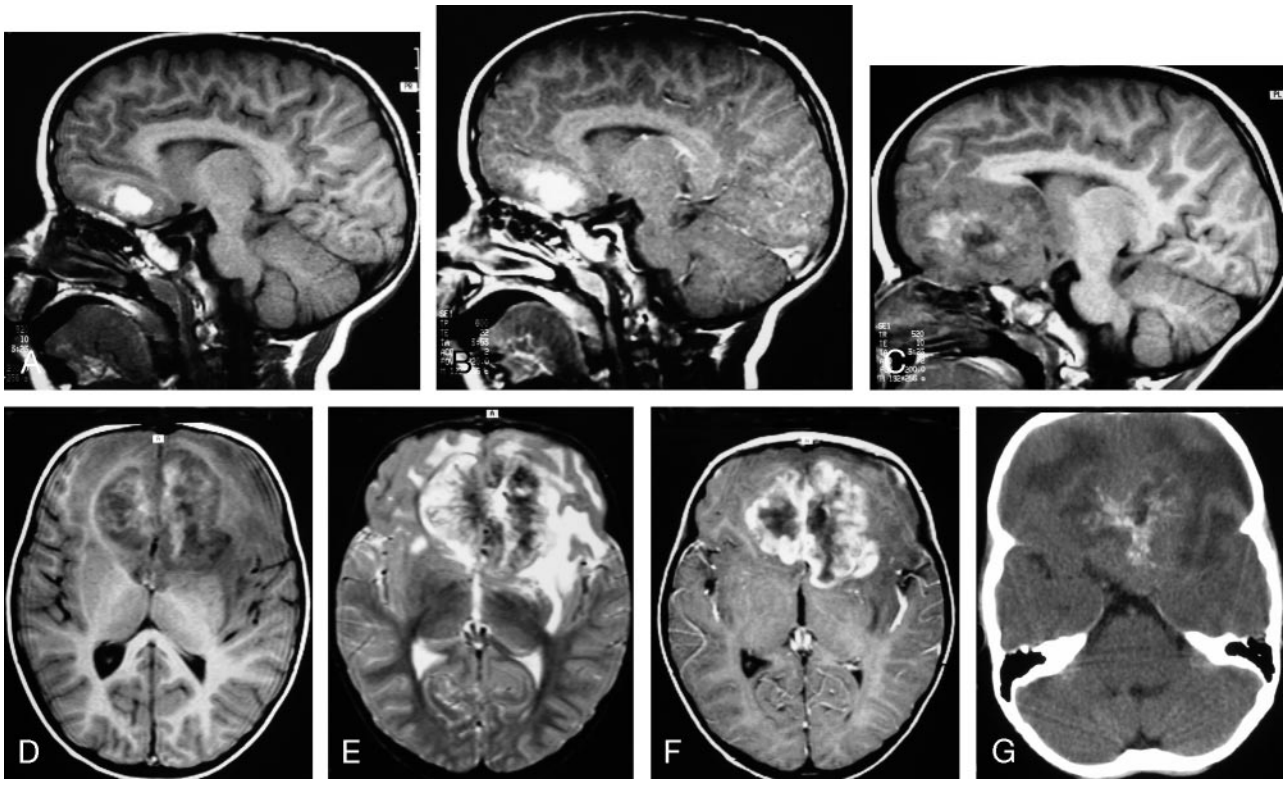

Fig 4. MR images of 3.4-year-old boy with a hemorrhagic AT/RT in the frontal lobe.

A, Sagittal (TR/TE, 520/10) MR image shows a hemorrhagic lesion in the inferior left frontal lobe.

B, Sagittal (TR/TE, 600/22) MR image shows edge enhancement of the lesion.

C and *D,* Sagittal (*C*) (TR/TE, 520/10) and axial (*D*) (TR/TE, 520/10) MR images obtained 7 months after *A*, *-B* show marked interval enlargement of the lesion, which has heterogeneous mixed low, intermediate, and high signal intensity involving the inferior portions of both frontal lobes.

E, Axial (TR/TE, 5700/90) MR image shows the tumor to have mixed low, intermediate, and high signal intensity, with evidence of edema in the surrounding brain tissue.

F, Axial (TR/TE, 600/22) MR image shows prominent heterogeneous contrast enhancement of the tumor with irregular lobulated margins. This patient underwent partial resection of the AT/RT, subsequently had disseminated leptomeningeal tumor, and died 3.3 years after surgery/initial diagnosis.

G, Axial CT image shows the lesion to have intermediate attenuation with multiple calcifications and zones of low attenuation.

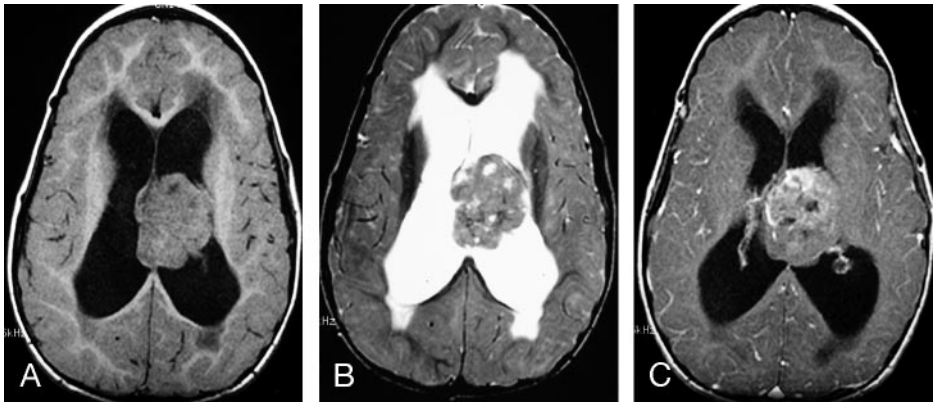

Fig 5. MR images of a 4-year-old girl with a constitutional ring 22 chromosome and AT/RT involving the septum pellucidum, with extension into the lateral ventricles.

A, Axial (TR/TE, 450/18) MR image shows the tumor to have intermediate signal intensity with several small zones of low signal intensity.

B, Axial (TR/TE, 4000/105) MR image shows the tumor to have heterogeneous predominantly intermediate-to-slightly-high signal intensity that is isointense to gray matter, as well as small zones of high and low signal intensity.

C, Axial (TR/TE, 450/31) MR image shows irregular heterogeneous contrast enhancement of less than two thirds of the primary AT/RT. This patient had subtotal resection of the tumor and subsequently had locally recurrent disease and disseminated leptomeningeal tumor. She died 14 months after surgery/initial diagnosis.

aging evidence of disseminated tumor in the leptomeninges (Fig 3). One patient had evidence of tumor in the intracranial leptomeninges, and 3 had evidence of disseminated tumor in both the spinal and intracranial leptomeninges. A 4-month-old patient with intracranial AT/RT involving the pineal gland, tectal plate, and vermis (Fig 6) also had a contemporaneous malignant rhabdoid tumor in the left kidney.

Tumor Size

At diagnosis, AT/RTs ranged from 1.2 to 6 cm superoinferiorly (mean, 3.6 cm; median, 3.7 cm) by 1.3–7 cm transversely (mean, 3.8 cm; median, 3.6 cm), and by 1.2–9 cm anteroposteriorly (mean, 3.9 cm; median, 3.3 cm) (Table 3). The smallest tumor was located in the midbrain (Fig 3), and the largest lesions were located in the frontal lobe (Fig 4).

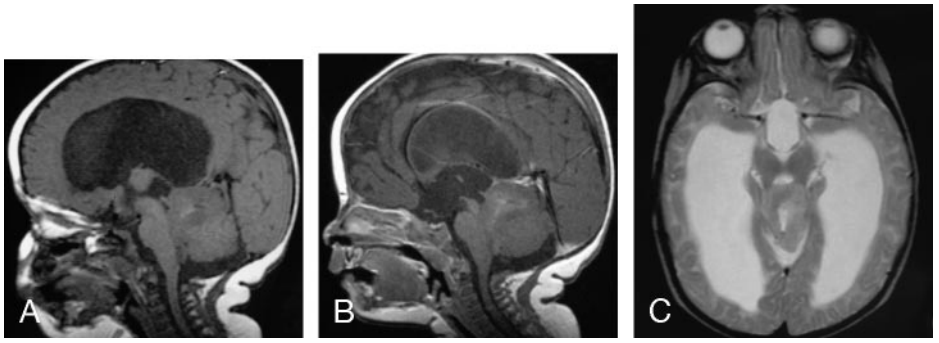

Fig 6. MR images of a 4-month-old female infant with a germ-line mutation of the hSNF5/INI1 gene with synchronous AT/RT, showing contiguous involvement of the pineal gland, dorsal midbrain, and upper cerebellum and a malignant rhabdoid tumor involving the left kidney.

A, Sagittal (TR/TE, 570/14) MR image shows the tumor to have predominantly intermediate signal intensity with several small zones of high signal intensity.

B, Sagittal (TR/TE, 750/22) MR image shows only minimal contrast enhancement in less than one third of the tumor.

C, Axial (TR/TE, 3710/105) MR image shows the tumor to have intermediate-to-slightly-high signal intensity that is isointense to gray matter, as well as a small zone of high signal intensity.

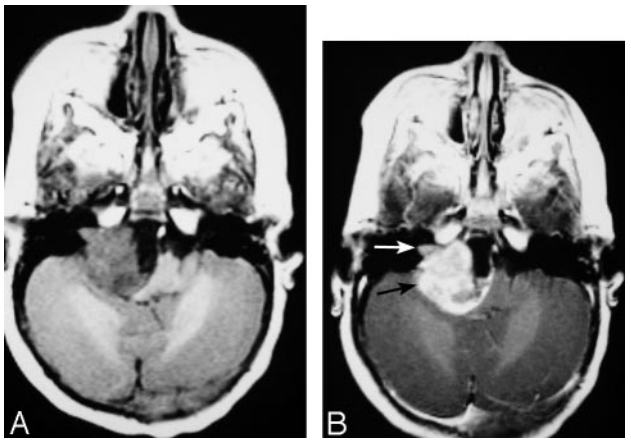

Fig 7. MR images of a 10-month-old female infant with an extra-axial AT/RT in the right cerebellopontine angle cistern, extending into the right internal auditory canal (*arrows*).

A, Axial (TR/TE, 550/14) MR image shows the tumor to have intermediate signal intensity with a zone of low signal intensity medially.

B, Axial (TR/TE, 600/22) MR image shows prominent enhancement of the solid portion of the lesion. This patient had subtotal resection followed by chemotherapy and died 1 month after surgery from sepsis related to immunosuppression from chemotherapy.

Preoperative MR Imaging Signal-Intensity Characteristics

Short TR/Short TE Images. On short TR images, AT/RT typically had heterogeneous intermediate signal intensity with zones of low ($n = 7$), high ($n = 1$), or both low and high ($n = 4$) signal intensity, resulting from cystic and/or necrotic regions, hemorrhage, or both, respectively (Figs 1, 2, 4, 5, and **7**). Foci of high signal intensity secondary to methemoglobin were small except for 1 lesion in the inferomedial left frontal lobe (Figs 2 and 4). One of the hemorrhagic lesions was initially thought to have been a hemorrhagic infarct versus hemorrhage secondary to a cavernous angioma (Fig 4). Subsequent MR imaging 7 months later showed a large intra-axial lesion involving both frontal lobes (Fig 4).

FLAIR Images. FLAIR images of AT/RT before surgery were available for review for 6 patients. Solid portions of AT/RT had intermediate signal intensity that was isointense ($n = 4$), isointense and slightly hyperintense ($n = 1$), or slightly hyperintense ($n = 1$) relative to gray matter (Figs 8 and 9 and Table 3).

Long TR/Long TE Images. On long TR/long TE images, solid portions of AT/RT typically had heterogeneous intermediate-to-slightly-high signal intensity that was isointense ($n = 6$), or slightly hyperintense ($n = 7$), and mixed isointense and slightly hyperintense relative to gray matter (Figs 1–6, 8, 9 and Table 3).

Small zones of low signal intensity were also seen in 5 lesions secondary to blood products ($n = 4$) or calcifications ($n = 1$) (Figs 2 and 4). Zones of high signal intensity comparable to CSF were seen in 12 of 13 tumors secondary to cystic/necrotic zones with ($n = 5$) or without ($n = 7$) hemorrhage (Figs 1, 2, 4–6, 8, 9). Cystic and/or necrotic tumor zones were <2 cm in 8 patients and >2 cm in 4 patients. Signal intensity heterogeneity was related to the relative proportions of cystic/necrotic zones and/or hemorrhage that were also seen on the short TR images. Reports from light microscopy of tumor samples described histologic findings of necrosis and hemorrhage in 10 and 4 of the tumors, respectively.

DWI and ADC Images. Four patients in this series had preoperative MR imaging that included DWI and ADC imaging. All 4 of these AT/RTs showed hyperintense signal intensity on DWI and hypointense signal intensity on ADC images relative to normal brain parenchyma, indicating restricted diffusion within these tumors (Fig 9 and Table 3).

Proton MR Spectroscopy. Proton MR spectra were available for review for 1 AT/RT before surgery and for 2 residual tumors after partial resection. All 3 AT/RTs showed elevated levels of choline and decreased *N*-acetylaspartate.

CT Images. Preoperative CT scans were available for review for 6 patients. Solid portions of the lesions had intermediate attenuation similar to ($n = 3$) or slightly higher ($n = 3$) than that of gray matter (Figs 1 and 4). Zones of low attenuation secondary to cystic necrotic changes were seen in all 6 AT/RTs. Calcifications were observed in 3 of the 6 lesions scanned with CT (Fig 4).

Findings on Contrast-Enhanced MR Images. All except 1 AT/RT showed contrast enhancement (Fig 8). Regarding the 12 AT/RT that showed contrast enhancement, the fraction of tumor volume showing enhancement was greater than two thirds in 7 patients (58%), between one third and two thirds in 4 (33%), and less than one third in 1 (9%) (Figs 1–7, 9). The enhancement pattern was most often heterogeneous ($n = 11$, 84%), and homogeneous in only one (6%). Portions of the enhancing margins of AT/RT were ill-defined in 3 patients (Figs 2 and 4). Abnormal enhancement in the intracranial leptomeninges representing disseminated tumor was found in 4 patients at the time of diagnosis (Fig 3).

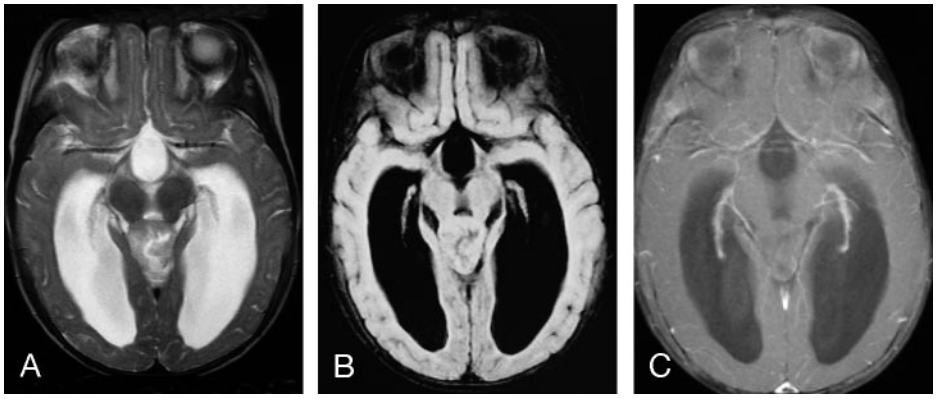

Fig 8. MR images of an 8-month-old female infant with AT/RT involving the pineal gland

A, Axial (TR/TE, 4000/105) MR image shows the tumor to have heterogeneous intermediate-to-slightly-high signal intensity with regions that are isointense and slightly hyperintense to gray matter, as well as a small zone of high signal intensity.

B, Axial FLAIR (TR/TE/TI, 9000/119/2200) MR image shows the tumor to have mostly intermediate signal intensity that is isointense to gray matter.

C, Axial (TR/TE, 800/20) fat-suppressed MR image with magnetization transfer shows no contrast enhancement of the primary lesion. This patient had subtotal resection of the primary lesion followed by chemotherapy. The patient had subsequent local recurrence and disseminated leptomeningeal tumor and died 7 months after initial diagnosis.

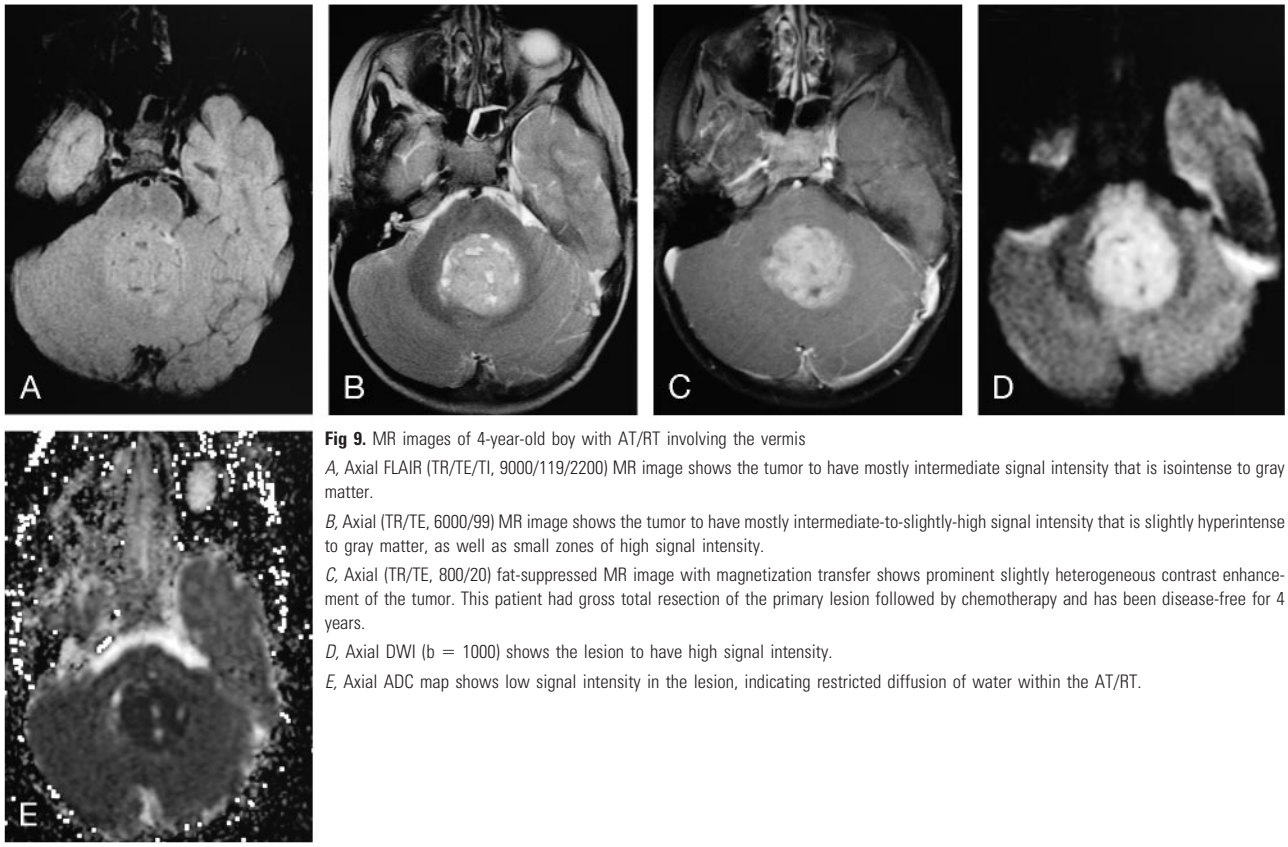

Fig 9. MR images of 4-year-old boy with AT/RT involving the vermis

A, Axial FLAIR (TR/TE/TI, 9000/119/2200) MR image shows the tumor to have mostly intermediate signal intensity that is isointense to gray matter.

B, Axial (TR/TE, 6000/99) MR image shows the tumor to have mostly intermediate-to-slightly-high signal intensity that is slightly hyperintense to gray matter, as well as small zones of high signal intensity.

C, Axial (TR/TE, 800/20) fat-suppressed MR image with magnetization transfer shows prominent slightly heterogeneous contrast enhancement of the tumor. This patient had gross total resection of the primary lesion followed by chemotherapy and has been disease-free for 4 years.

D, Axial DWI (b = 1000) shows the lesion to have high signal intensity.

E, Axial ADC map shows low signal intensity in the lesion, indicating restricted diffusion of water within the AT/RT.

Patient Outcomes and Findings on Postoperative Contrast-Enhanced MR Images. Thirteen patients (76%) have died from 1 month to 12.5 years (mean, 2.3 years; median, 1.3 years) after diagnosis. Only 3 of the 13 patients who died had undergone gross total resections (Table 1). Other factors associated with a poor prognosis were young age at diagnosis and presence of disseminated leptomeningeal tumor. Patients who died had mean and median ages of 2.4 and 1.7 years at diagnosis, respectively, compared with the surviving patients whose mean and median ages were 8.1 and 7 years at diagnosis, respectively ($P = .009$, Mann-Whitney U test). Ten of the 13 deceased patients had MR imaging evidence of disseminated leptomeningeal tumor at the time of diagnosis ($n = 4$) or in the subsequent postoperative period ($n = 6$). The 4 patients who had disseminated tumor in the leptomeninges at diagnosis died from 4 months to 5.1 years (mean, 2.1 years) later. Only 1 of these patients had a reported gross total resection of the primary tumor. The other 6 deceased patients with disseminated disease had evidence of subarachnoid tumor on MR images from 3 months to 2.8 years (mean, 1.1 years) after surgery and earlier negative findings on imaging examinations. Only 2 of these patients had gross total resection of the primary tumors. These 6 patients also had MR imaging evidence of residual or locally recurrent tumor before ($n = 3$), contemporaneous with ($n = 2$), or after ($n = 1$) detection of disseminated leptomeningeal tumor with MR imaging. One of these patients also had extension of disseminated intracranial subarachnoid tumor into the peritoneal cavity via a ventricu-

loperitoneal shunt. The presence of disseminated leptomeningeal tumor seen with MR imaging was significantly associated with patients' deaths ($P = .002$, Fisher exact test). For patients who died with MR imaging evidence of leptomeningeal tumor, contemporaneous CSF cytology was positive in 56%. None of the patients who died had CSF cytology positive for tumor cells without MR imaging evidence of disseminated tumor.

Of the 3 remaining deceased patients, 1 died from sepsis related to immunosuppression from chemotherapy. Another patient was a 4-month-old female infant with a germ-line mutation who had intracranial AT/RT as well as a malignant rhabdoid tumor in the left kidney. This patient died 6 weeks after diagnosis from metastatic pulmonary lesions from the malignant renal rhabdoid tumor (Fig 6). The third patient was 3.4 years old at diagnosis and died 12.5 years later after 3 local recurrences, despite 3 surgeries and multiple cycles of chemotherapy.

The 4 patients who are alive have follow-up intervals ranging from 4 to 11.5 years (mean, 8.4 years; median, 9 years) after surgery. Surviving patients ranged from 3.2 to 15 years at the time of diagnosis. Three surviving patients had gross total surgical resection, and the other had a subtotal resection. One of the surviving patients had postsurgical radiation, and 3 had both radiation and chemotherapy. The 3 patients who had gross total resections have had no evidence of residual or locally recurrent tumor or disseminated neoplasm by MR imaging or CSF cytology in follow-up periods ranging from 4 to 11.5 years (mean, 8.5 years) after surgery. The single surviving patient who had a subtotal resection has been disease-free 7 years after a complete response for minimal residual local disease.

Discussion

AT/RTs are rare malignant intracranial tumors, representing only 1.3% of primary CNS tumors in the pediatric population and 6.7% of CNS tumors in children younger than 2 years.[2] Malignant rhabdoid tumors can occur in many locations in the body, though the kidney and CNS are the most common primary sites.[3] Within the CNS, 38%–65% have been reported to be infratentorial, 27%–62% in supratentorial locations, and 4%–8% occurring in multiple CNS sites at diagnosis.[1,3,9]

Rhabdoid cells in AT/RT observed with light microscopy are often plump with eccentric round nuclei containing prominent nucleoli within fibrillary or granular eosinophilic cytoplasm, though rhabdoid tumor cells can also be small and spindle-shaped with ovoid nuclei or large, containing nuclei with wrinkled margins.[1,3,5,11] Abundant mitotic figures, necrosis, hemorrhage, and ill-defined margins with adjacent brain are common histologic feature seen in AT/RT.[1,3,5,11] In addition to the rhabdoid tumor cells, intracranial AT/RTs often contain varying percentages of PNET cells, malignant mesenchymal spindle-shaped cells, and cells with epithelial differentiation.[1,3,5,11] The presence of these diverse elements accounts for naming these neoplasms "AT/RT."[3,11,12] Despite the presence of multiple cellular elements in these tumors, AT/RTs lack germ cell and tissue differentiation associated with malignant teratomas.[3,5] In addition, AT/RTs do not show immunoreactivity to epitopes associated with germ cell tumors such as human chorionic gonadotropin, placental alkaline phosphatase, and alpha-fetoprotein.[3,5] Up to 70% of AT/RTs contain areas that histologically resemble PNET.[1,3,4,7,11] This latter feature has caused erroneous diagnosis of AT/RT as PNET in the past.[3,4] Positive reactions to neural antibodies such as neurofilament protein and glial fibrillary acid protein may be present in both PNET and AT/RT.[3] Rhabdoid cells in AT/RT, however, typically express epithelial membrane antigen, vimentin, and smooth-muscle actin, which can provide discrimination from PNET and germ cell tumors.[3] Epithelial cells express keratin, whereas desmin is often expressed in the mesenchymal components.[3,5]

A variety of cytogenetic abnormalities involving chromosome 22 have been found in AT/RT, typically resulting in monosomy 22 or deletions involving band 22q11.2.[1,3,5-9,10-13,15,16] Deletion of 22q11.2, most often detected by fluorescence in situ hybridization, results in loss of the hSNF5/INI1/SMRCB1/BAF47 gene.[4-7,12,13,16] Molecular genetic analysis of tumor tissue demonstrates deletion and/or mutation of hSNF5/INI1 in approximately 70% of AT/RTs.[4-7,12,13,16] Inactivation of this gene is also diagnostic of rhabdoid tumors of the kidney and other extrarenal sites.[8,12,13,16] The hSNF5/INI1 gene codes for an essential component of the SWI/SNF ATP-dependent chromatin remodeling complex.[4,7,10,12,13] Functional studies have shown that hSNF5/INI1 may activate and repress target genes, though the specific role of this gene in tumor suppression has not yet been elucidated.[4,7,10,12,13] All 7 AT/RTs tested in our study had deletions and/or mutations of this tumor-suppressor gene, and all 4 patients tested had loss of nuclear expression of the protein by immunohistochemistry, confirming the diagnosis of AT/RT.

In addition to acquired somatic mutations involving the hSNF5/INI1 gene in AT/RT, germ-line mutations of this gene have also been reported in some patients, including those with synchronous intracranial AT/RT and renal and/or other extrarenal malignant rhabdoid tumors.[13,16-20] Germ-line mutations or deletions result in predisposition to developing these malignant tumors at 1 or more sites.[6,13,16-20] The 4-month-old patient in our series who had contemporaneous intracranial AT/RT and a malignant renal rhabdoid tumor was found to have a germ-line mutation of the hSNF5/INI1 gene. Despite the fact that both the intracranial AT/RT and the malignant renal rhabdoid tumor had inactivation of both hSNF5/INI1 tumor-suppressor genes; the intracranial tumor contained rhabdoid, PNET, epithelioid, and mesenchymal tumor cells and showed immunoreactivity to GFAP and NFP, whereas the renal tumor contained only rhabdoid tumor cells and was not immunoreactive to GFAP and NFP. These differing features indicate that these 2 tumors are distinct primary lesions rather than metastases, because the latter would have similar histologic features and immunohistochemical profiles.[16] Germ-line mutations involving the hSNF5/INI1 gene have also been reported in monozygotic twins.[18] One twin had disseminated AT/RT, and the other had a tumor mimicking medulloblastoma with immunoreactivity to vimentin and epithelial membrane antigen.[18] In both twins, DNA sequence abnormalities were found involving the same exon of the hSNF5/INI1 gene on chromosome 22.[18] It has been recommended that patients with demonstrated mutations of the hSNF5/INI1 gene in AT/RT have analysis of blood samples to exclude the possibility and implications of constitutional mutations.[20]

The preoperative MR imaging signal-intensity characteristics on short TR and long TR/long TE images and contrast-enhancement features of AT/RTs were usually nonhomogeneous, secondary to the heterogeneous cellular populations in these tumors as well as the frequent presence of necrosis, hemorrhage, and/or calcifications. Similar MR imaging findings have been reported in multiple prior small series of intracranial AT/RT.[21-36] Solid portions of AT/RT typically had intermediate-to-slightly-high signal intensity on FLAIR and long TR/long TE images that were isointense and/or slightly hyperintense relative to gray matter. In addition, AT/RTs were shown to have restricted diffusion. The MR imaging findings for AT/RT on long TR/long TE, FLAIR, and DWI are similar to those reported for PNET and are likely related to overlapping histologic features of these hypercellular tumors containing neoplastic cells with high nuclear-to-cytoplasmic ratios and small extracellular spaces.[37,38] These MR imaging features for AT/RT and PNET have been reported to occur infrequently in other primary pediatric glial tumors involving the brain.[37]

In the current study, calcifications within AT/RT were seen in half of the patients who underwent preoperative CT. Similar CT findings have been reported previously.[27,29,32] AT/RTs show various patterns and degrees of gadolinium contrast enhancement, which are features that have been reported for PNET.[38,39] In addition, the proton MR spectra of AT/RT and PNET typically show elevated levels of choline and decreased *N*-acetylaspartate.[38,40] Similarities of many imaging features of AT/RT with PNET likely prevent reliable discrimination of these neoplasms based solely on MR imaging data.

The presence of disseminated leptomeningeal tumor at diagnosis/staging and later has been associated with a poor prognosis in patients with AT/RT.[1,3,5,20] Leptomeningeal dissemination of tumor at diagnosis/initial staging has been previously reported in 21%–34% of patients with AT/RT by using myelography or gadolinium-enhanced MR imaging and CSF cytology.[3,9,10] Subsequent data from the Children's Cancer Group and AT/RT registry have suggested that the incidence of leptomeningeal dissemination at diagnosis/initial staging is approximately 15%.[20] In the current report, disseminated tumor in the leptomeninges was seen with MR imaging in 24% of patients at diagnosis/initial staging and occurred in another 35% from 4 months to 2.8 years (mean, 1 year) after surgery and earlier imaging examinations with negative findings. Similar frequencies of disseminated tumor have been reported for PNET/MB.[38,41] Ten of the 13 patients with AT/RT who died had MR imaging evidence of disseminated leptomeningeal tumor, including 7 (54%) with residual postoperative tumor. Five patients who died also had progressive enlargement of residual or locally recurrent tumor documented with MR imaging. Similar relapse and disease progression patterns of intracranial AT/RT after surgery have been reported.[1,3,9,10] CSF cytology was positive in only 56% of patients with MR imaging evidence of disseminated leptomeningeal tumor who died. These results are similar to those of a previous report that found that postoperative MR imaging had greater diagnostic accuracy in the early detection of disseminated leptomeningeal medulloblastoma, compared with CSF cytology.[41]

The prognosis of patients with AT/RT is dismal, with reported mean survival rates in the range of 6–15 months.[1,3,5,9,10,20] Gross total resection has been suggested to improve median patient survival rates, compared with those having lesser resection.[20] Gross total or near-complete resections of AT/RT, however, can be performed in fewer than half of patients with AT/RT because of large tumor sizes at diagnosis in young patients and surgically challenging locations.[9,20] Patients with intracranial AT/RT have been treated with different chemotherapy protocols, which have been mostly ineffective.[1,3,5,9,10,20] Moderate responses of AT/RT to high-dose myeloablative chemotherapy followed by autologous bone marrow transplantation or stem cell rescue have been observed, though long-term outcome data are not available.[20] Older patients who received chemotherapy and radiation therapy have a higher likelihood of survival compared with those who received chemotherapy alone.[20] Packer et al[20] reported that there is no effective treatment for children with disseminated AT/RT at diagnosis or for those with tumors initially nonresponsive to chemotherapy.[20] Multi-institutional treatment protocols specifically designed for AT/RT are in development within the Children's Oncology Group.[20]

Conclusion

AT/RTs are rare malignant intracranial neoplasms usually occurring in young children. AT/RTs have aggressive growth with high potential for dissemination within the CNS. These tumors have been misdiagnosed in the past as PNET/MB because of frequent overlapping histologic and imaging features. AT/RT can now be distinguished from PNET/MB by using specific immunohistochemical markers (EMA, vimentin, actin, hSNF5/INI1) and mutation analysis. Confirmation of the diagnosis of AT/RT is important because these tumors typically have a poor prognosis that is worse than that in PNET/MB, necessitating new intensified therapies. AT/RT was found to be mostly intra-axial (94%) except for 1 extra-axial lesion seen in the cerebellopontine angle cistern. AT/RT can be infra- and/or supratentorial. The unenhanced and enhanced MR imaging features of AT/RT are often variable secondary to cystic/necrotic changes and/or hemorrhage. Disseminated tumor in the leptomeninges was seen with MR imaging in 24% of patients at diagnosis/initial staging and occurred in another 35% from 4 months to 2.8 years after surgery and earlier imaging examinations with negative findings. The overall 1-year and 5-year survival probabilities were 71% and 28%, respectively. Factors associated with poor prognosis were young age at diagnosis ($P = .009$) and MR imaging evidence of disseminated leptomeningeal tumor ($P = .002$).

References

1. Burger PC, Yu I-T, Friedman HS, et al. **Atypical teratoid/rhabdoid tumor of the central nervous system: a highly malignant tumor of infancy and childhood frequently mistaken for medulloblastoma—a pediatric oncology study.** *Am J Surg Pathol* 1998;22:1083–92
2. Rickert CH, Paulus W. **Epidemiology of central nervous system tumors in childhood and adolescence based on the new WHO classification.** *Childs Nerv Syst* 2001;17:503–11
3. Rorke LB, Packer RJ, Biegel JA. **Central nervous system atypical teratoid/rhabdoid tumors of infancy and childhood: definition of an entity.** *J Neurosurg* 1996;85:56–65
4. Biegel JA, Fogelgren B, Zhou JY, et al. **Mutations of the INI1 rhabdoid tumor suppressor gene in medulloblastomas and primitive neuroectodermal tumors of the central nervous system.** *Clin Cancer Res* 2000;6:2759–63

5. Bruch LA, Hill A, Cai DX, et al. **A role for fluorescence in situ hybridization detection for chromosome 22q dosage in distinguishing atypical teratoid/rhabdoid tumors from medulloblastoma/central primitive neuroectodermal tumors.** *Hum Pathol* 2001;32:156–62
6. Biegel JA, Zhou JY, Rorke LB, et al. **Germ-line and acquired mutations of INI1 in atypical teratoid and rhabdoid tumors.** *Cancer Res* 1999;59:74–79
7. Judkins AR, Mauger J, Rorke LC, et al. **Immunohistochemical analysis of hSNF5/INI1 in pediatric CNS neoplasms.** *Am J Surg Pathol* 2004;28:644–50
8. Perry A, Fuller CE, Judkins AR, et al. **INI1 expression is retained in composite rhabdoid tumors, including rhabdoid meningiomas**. *Mod Pathol* 2005;18: 951–58
9. Hilden JH, Meerbaum S, Burger P, et al. **Central nervous system atypical teratoid/rhabdoid tumor: results of therapy in children enrolled in a registry.** *J Clin Oncol* 2004;22:2877–84
10. Tekautz TM, Fuller CE, Blaney S, et al. **Atypical teratoid/rhabdoid tumors (AT/RT): improved survival in children 3 years of age and older with radiation therapy and high-dose alkylator-based chemotherapy.** *J Clin Oncol* 2005;23: 1491–99
11. Parwani AV, Stelow EB, Pambuccian SE, et al. **Atypical teratoid/rhabdoid tumor of the brain: cytopathologic characteristics and differential diagnosis.** *Cancer* 2005;105:65–70
12. Biegel JA. **Cytogenetics and molecular genetics of childhood brain tumors.** *Neuro-oncol* 1999;1:139–51
13. Biegel JA, Tan L, Zhang F, et al. **Alterations of the hSNF5/INI1 gene in central nervous system atypical teratoid/rhabdoid tumors and renal and extrarenal rhabdoid tumors.** *Clin Cancer Res* 2002;8:3461–67
14. Kaplan EL, Meier P. **Nonparametric estimation from incomplete observations.** *J Am Stat Assoc* 1958;53:457–81
15. Rubio A. **March 1997: 4 year old girl with ring chromosome 22 and brain tumor**. *Brain Pathol* 1997;7:1027–28
16. Biegel JA, Fogelgren B, Wainwright LM, et al.. **Germline INI1 mutation in a patient with a central nervous system atypical teratoid tumor and renal rhabdoid tumor.** *Genes Chromosomes Cancer* 2000;28:31–37
17. Taylor MD, Gokgoz N, Andrulis IL, et al. **Familial posterior fossa brain tumors of infancy secondary to germ-line mutation of the HSNF5 gene.** *Am J Hum Genet* 2000;66:1403–06
18. Fernandez C, Bouvier C, Sevenet N, et al. **Congenital disseminated malignant rhabdoid tumor and cerebellar tumor mimicking medulloblastoma in monozygotic twins: pathologic and molecular diagnosis.** *Am J Surg Pathol* 2002;26:266–70
19. Sevenet N, Sheridan E, Amram D, et al.. **Constitutional mutations of the hSNF5/INI1 gene predispose to a variety of cancers.** *Am J Hum Genet* 1999;65: 1342–48
20. Packer RJ, Biegel JA, Blaney S, et al. **Atypical teratoid/rhabdoid tumor of the central nervous system: report on workshop.** *J Pediatr Hematol Oncol* 2002;24: 337–42
21. Hanna SL, Langston JW, Parham DM, et al. **Primary malignant rhabdoid tumor of the brain: clinical, imaging, and pathologic findings.** *AJNR Am J Neuroradiol* 1993;14:107–15
22. Caldemeyer KS, Smith RR, Azzarelli B, et al. **Primary central nervous system malignant rhabdoid tumor: CT and MR appearance simulates a primitive neuroectodermal tumor.** *Pediatr Neurosurg* 1994;21:232–36
23. Munoz A, Carrasco A, Munoz MJ, et al. **Cranial rhabdoid tumor with marginal tumor cystic component and extra-axial extension**. *AJNR Am J Neuroradiol* 1995;1727–28
24. Howlett DC, King AP, Jarosz JM, et al. **Imaging and pathologic features of primary malignant rhabdoid tumors of the brain and spine.** *Neuroradiology* 1997;39:719–23
25. Martinez-Lage JF, Nieto A, Sola J, et al. **Primary malignant rhabdoid tumor of the cerebellum.** *Childs Nerv Syst* 1997;13:418–21
26. Zuccoli G, Izzi G, Bacchini E, et al. **Central nervous system atypical teratoid/rhabdoid tumour of infancy: CT and MR findings.** *Clin Imaging* 1999;23: 356–60
27. Evans A, Ganatra R, Morris SJ. **Imaging features of primary malignant rhabdoid tumor of the brain.** *Pediatr Radiol* 2001;31:631–33
28. Arrazola J, Pedrosa I, Mendez R, et al. **Primary malignant rhabdoid tumour of the brain in an adult.** *Neuroradiology* 2000;42:363–67
29. Bambakidis NC, Robinson S, Cohen, et al. **Atypical teratoid/rhabdoid tumors of the central nervous system: clinical, radiographic and pathologic features.** *Pediatr Neurosurg* 2002;37:64–70
30. Dang T, Vassilyadi M, Michaud J, et al. **Atypical teratoid/rhabdoid tumors.** *Childs Nerv Syst* 2003;19:244–48
31. Fenton LZ, Foreman NK. **Atypical teratoid/rhabdoid tumor of the central nervous system in children: an atypical series and review.** *Pediatr Radiol* 2003;33: 554–58
32. Arslanoglu A, Aygun N, Tekhtani D, et al. **Imaging findings of CNS atypical teratoid/rhabdoid tumors.** *AJNR Am J Neuroradiol* 2004;25:476–80
33. Lee YK, Choi CG, Lee JH. **Atypical teratoid/rhabdoid tumor of the cerebellum: report of two infantile cases.** *AJNR Am J Neuroradiol* 2004;25:481–83
34. Gandhi CD, Kreiger MD, McComb JG. **Atypical teratoid/rhabdoid tumor: an unusual presentation.** *Neuroradiology* 2004;46:834–37
35. Cheng YC, Lirng JF, Chang FC, et al. **Neuroradiological findings in atypical teratoid/rhabdoid tumor of the central nervous system.** *Acta Radiol* 2005;46: 89–96
36. Reinhardt D, Behnnke-Mursch J, Weib E, et al. **Rhabdoid tumors of the central nervous system.** *Childs Nerv Syst* 2000;16:228–34
37. Erdem E, Zimmerman RA, Haselgrove JC, et al. **Diffusion-weighted imaging and fluid-attenuated inversion recovery imaging in the evaluation of primitive neuroectodermal tumors.** *Neuroradiology* 2001;43:927–33
38. Koeller KK, Rushing EJ. **Medulloblastoma: a comprehensive review with radiologic-pathologic correlation.** *RadioGraphics* 2003;23:1613–37
39. Meyers SP, Kemp SS, Tarr RW. **MR imaging features of medulloblastomas.** *AJR Am J Roentgenol* 1992;158:859–65
40. Girard N, Wang ZJ, Erbetta A, et al. **Prognostic value of proton MR spectroscopy of cerebral hemisphere tumors in children.** *Neuroradiology* 1998;40: 121–25
41. Meyers SP, Wildenhain SL, Chang JK, et al. **Postoperative evaluation for disseminated medulloblastoma involving the spine: contrast-enhanced MR findings, CSF cytologic analysis, timing of disease occurrence, and patient outcomes.** *AJNR Am J Neuroradiol* 2000;21:1757–65